

Spatial Textile Hybrids: Computing a Self-Forming behavior

Jorge Christie

École Polytechnique Fédérale de Lausanne, Switzerland

<http://christie.cl>

jorge.christie@gmail.com

Abstract. This paper introduces a novel approach for generating self-forming textile hybrid structures based on the actuation of pre-stressed textiles with in-space robotic 3D printing. By revising the transit from material experimentation to the definition of geometrical models and fabrication processes, the so-called “Spatial Textile Hybrids” are presented. With the aim of visualizing the potential of this technique for designers, a preliminary environment of computational tools is developed, ranging from printing a path prediction algorithm to form-finding simulation and printing path designing. By contrasting a series of physical prototypes with digitally form-found samples, the strengths and weaknesses of the process are exposed and recommendations for further development issued.

Keywords. Textile Hybrid; 4D printing; Robotic 3D Printing; Force-active.

Introduction

Due to the complex network of forces that usually converge on textile hybrid structures, the predictability and control over the design of the final form tends to be elusive, computationally demanding and often requires the existence of a physical prototype as starting point. This paper presents a novel, highly predictable and simple approach for generating textile hybrid structures based on the actuation of pre-stressed fabrics with in-space robotic 3D printing. The dialogue of forces between the tension-active and bending-active members of the hybrid structure is explored on its capacity for inducing a transformation of the system from an initially bi-dimensional pre-stressed configuration to a final three-dimensional one when released.

In general terms, this paper exposes the process of translation of a physical phenomenon: the morphological transformation of a textile hybrid system, into a Computational Design environment. Based on its attentive observation, its abstraction and decoding, a behavioral hypotheses could be issued and, consequently, a set of parametric design tools implemented to visualize the design potential of this technique.

This paper is based on the research “Spatial Textile Hybrids: Self forming 3D Printing-induced structures” realized during the MAS in Architecture and Digital Fabrication at ETH Zürich under the tutorship of Prof. Fabio Gramazio and Mathias Kohler and the advice of Luka Piskorec.

Spatial Textile Hybrids

For defining Spatial Textile Hybrid systems we should understand them from two main frameworks: as a force-active system and as an Additive Manufacturing technique.

At structural level, the term *Spatial Textile Hybrid* (STH) comes as an expansion of the definition of textile hybrid structure made by Lienhard, Ahlquist, Menges and Knippers (2013) where they describe it as “the interdependence of form and force of mechanically pre-stressed membranes and bending-active fiber-reinforced polymers”.

Textile hybrid's definition is, subsequently, an expansion of the more generic category of *hybrid* structures made by Heino Engel, referring to structures composed by two different mechanical systems combined to achieve new mechanical behavior (Engel 2001). 253

In all textile hybrid cases studied by this author (Lienhard et al. 2013, Ahlquist and Menges 2013, Thomsen et al. 2015, Kuma 2016), the tension-active elements meet the bending-active ones in a linear fashion, where the elastic beam actuates the textile in a boundary or a ridge condition [Fig. 1]. In this sense, we have added the term “Spatial” to the definition of STH in order to distinguish our approach from other textile hybrids. In STH, the spatial extrusion of the bending element establishes only a point contact with the textile, creating its own actuation logic and its distinguishable expression. Besides, is precisely this spatial condition and its topographic variation what enables to control local stiffness and, ultimately, the morphology of the system.

On the other hand, from the perspective of Additive Manufacturing, STHs share some logics with what is being called Programmable Matter or 4D printing (Tibbits 2013, Campbell et al. 2014). In short, 4D printing -as an extension of 3D printing- refers to the ability of material objects to change form and function after they are produced (Campbell 2014). Although usually associated to with multi-material 3D printing, what lays behind all transformations processes in 4D printing is a programmed force dialogue between materials with different properties. A usually highly expansive and environmentally sensitive material exerts forces against a stiffer one inducing morphological transformations on the system. Accordingly, the geometrical arrangement of these materials is what will define the direction and amplitude of that process (Tibbits et al. 2014). In this sense, the control over this transformation in time is provided by mathematical models that enables to solve *forward problems* as well as *inverse problems* (Gladman et al. 2016). A forward problem consists on the determination of a final desired shape from given conditions like a print path, material properties and stimulus properties. Contrariwise, an inverse problem would seek to determine the printing path and nozzle given a target form and stimulus.

Similarly, when aiming to become a design tool, STH technique should explore both problem scenarios; one where forms emerge from exploring certain printing path and material constraints, as well as seeking the printing path conditions for achieving a targeted form.



Figure 1

Left: Toroidal textile hybrid, Sean Ahlquist; center: Hybrid Tower, Thomsen et al.; right: grid deformation, Self-Forming Lab, MIT.

Methodology

In both framework references studied, the process of successfully transferring the behavior of complex force-active systems into a computational design environment, requires a multi-modal approach. Therefore, a workflow with constant feedback between design, fabrication, physical and numerical form-finding (and structural analysis when aimed to comply with certain mechanical performance) has to be implemented (Ahlquist, Menges 2013, Raviv et al. 2014). Ahlquist has pointed out as well the relevance of multi-scale prototyping due to the non-linearity of material behavior when scaled. In our case, we have fixed the scale of our physical prototypes to the capacities of the available fabrication facilities at the time of the realization of this research.

Although the steps followed by this research were nonlinear and successive findings would redefine or refine previous steps, the overall workflow can be synthesized in the following diagram [fig. 2]. This paper will concentrate primarily on the first four steps, which are the basis for eventual further developments on this technique, and will introduce one of the Computational Design tools as a proof of concept.

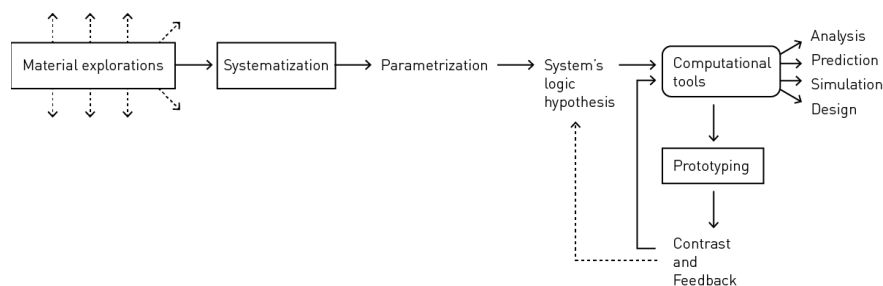


Figure 2
STH research workflow

Material exploration

As previously mentioned, this research emerges from an intense material exploration course. By an iterative process of testing, observing material behavior and adjusting procedures, we were able to progressively comprehend and control those phenomena [fig. 3].

Essentially, STHs consist on 2 different material-inherent mechanical systems, a tensile-active component: the pre-stressed fabric, and a bending-active component: the in-space robotically extruded ABS filament.

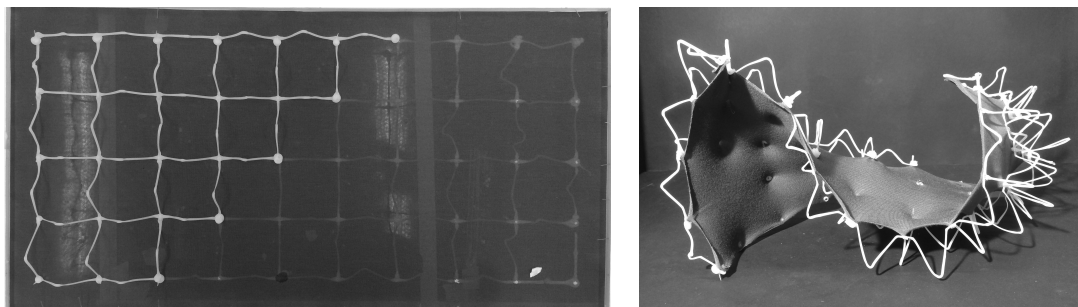


Figure 3

Early explorations in STH. Left: initial pre-stressed state in tension bed. Two side printing path can be appreciated; right: final released state.

The printing setup

The setup utilized was composed by a 6 axis Universal Robot UR-5 with a plastic filament extruder attached and a tension bed for stretching the fabric [fig 4]. The extruder is fed with a 3 mm \varnothing filament of HS-ABS and has small orientable fan in order to produce a fast cooling of the filament in the required position. On the other hand, the tension bed consists on a reinforced frame of 10 mm foam board -where the fabric is progressively pinned- and a series of distancers that enable printing in both sides. A free margin of 50 mm was left free to avoid border's wavy aberrations.

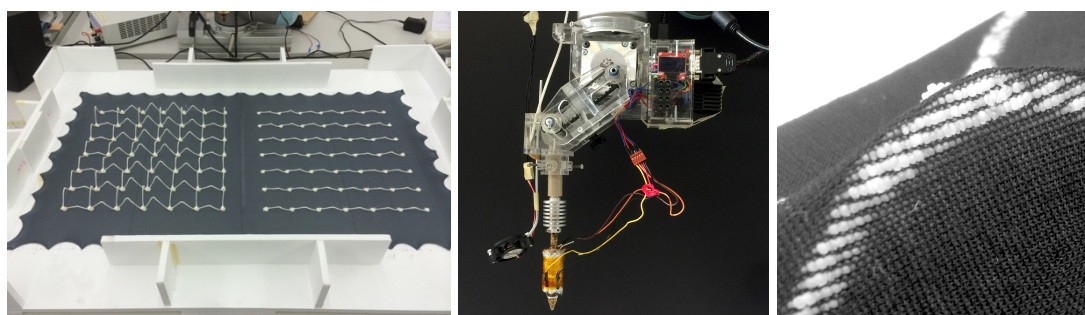


Figure 4

Left: two pre-released state samples (synclastic-variable curvature and anticlastic-constant curvature); center: filament extruder mounted on the UR-5 robot; right: detail of the mechanical bonding between filament and fabric.

The tensile -active component: the fabric

The fabric used for the prototypes was chosen under the following criteria: to have a high stretching ratio, to be as equally elastic on both directions as possible and to be resistant to high temperatures.

After several tests of available commercial fabrics we chose a “jersey”, which is a knitted fabric with a Stockinette pattern composed, in this case, of 90% viscose and 10% elastane. We measured a stretching factor of 1.76 on its weft direction and 1.6 on its warp direction and a resiliency factor of 1.03 and 1.04 respectively. The asymmetric behavior of the fabric was considered later on the definition of the computational tools.

The bending-active component: the extruded filament

One of the main advantages on using a robot for controlling the extrusion of thermoplastics, is the high degree of freedom that it offers for extruding in the tridimensional space. Was particularly this feature what enabled us to develop this technique.

The accomplishment of an optimal result with the extrusion is a function of adjusting the many variables that come together: the robot trajectory, speed and acceleration, the fusion temperature and the filament material. Concerning the robot trajectory, the best results were achieved by defining a trajectory sensitive to the different particularities of each step, controlling the on-and-off switching of the

extruder and introducing a precise waiting time to allow the bonding, cooling and clean take off from the contact point [fig. 5].

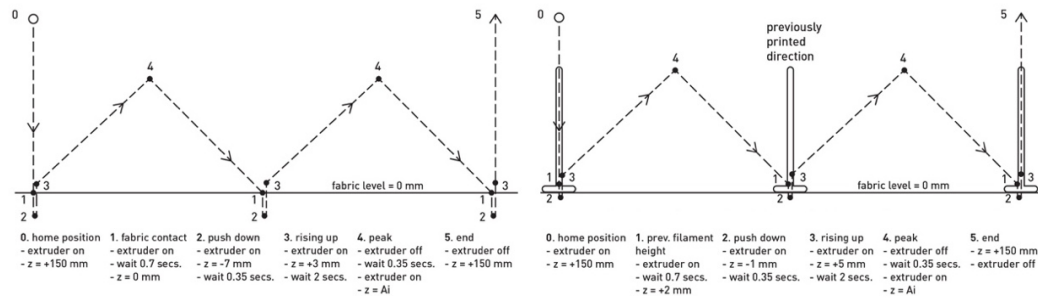


Figure 5
Robot printing path procedure. Left: first direction print path; right: second direction print path for synclastic surfaces.

From the material point of view, after trying PET, ABS and HS-ABS, we opted for the last one due to its clean and stable extrusion and its good bonding with the fabric.

Systematization

In general terms, the STHs can be topologically described as surface that has point contact with two series of normally oriented zig-zag shaped filaments correspondingly aligned to U and V surface coordinates. Using the analogy of a triangular waveform, we defined as Frequency (F) the distance between the contact points of filament and fabric and as Amplitude (A) the one between the summit of the triangular extrusion and the fabric [fig. 6].



Figure 6
Comparison of the geometric transformations of rows of samples with different A_i . Left: higher A_i ; right: lower A_i .

Additionally, two relevant topological variations of the system were identified: one side printing (U and V) and two side printing (U or V). Each topology defines a primitive, the first generating synclastic surfaces and the second generating anticlastic surfaces [fig. 7].

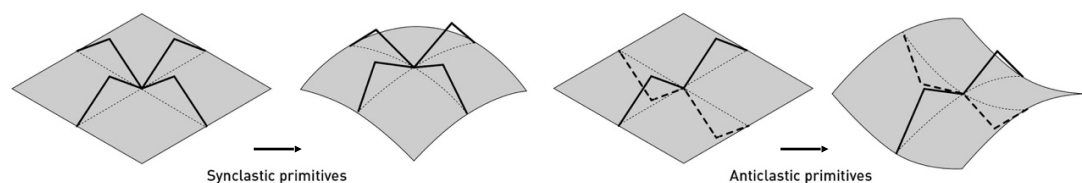


Figure 7
System's primitives. Left: synclastic primitive and transformation; right: anticlastic primitive and transformation.

With the aim of effectively comprehend and control the behavior of STH, it became imperative to simplify the system and to test impact of the variation of a single

parameter in the morphological transformation. Accordingly, we produced 2 series of 3 samples: a synclastic series and an anticlastic one. Both series were based on a square grid of 3x3 modules of 50 mm side. The only varying parameter was the Initial Amplitude (A_i), being 10, 20 and 40 mm. for each sample of a series. [fig 8].

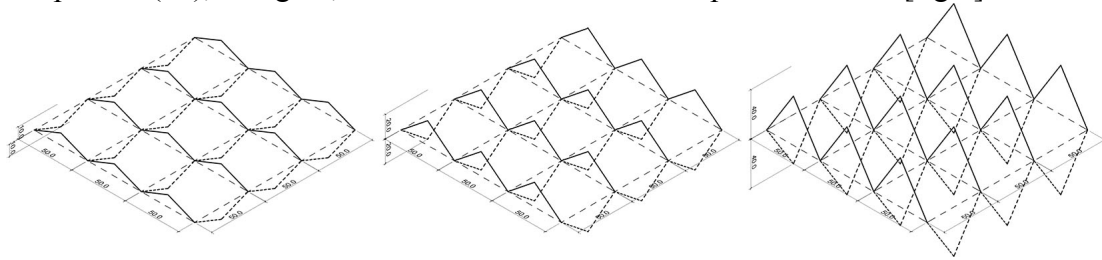


Figure 8

Printing path of the anticlastic series. From left to right: 10mm A_i , 20 mm A_i and 40 mm A_i .

All samples fabricated were measured on its initial “pre-release” state and on its final “released” state. The gathered data for each triangle of each sample was the effective Initial Amplitude (A_i), the final frequency (F_f) and the final angle at the peak point (δf). Concerning the production of the data table for comparing initial and final state, we assumed that the initial frequency (F_i) was precisely executed by the robot (50 mm) and that the triangles were always isosceles.

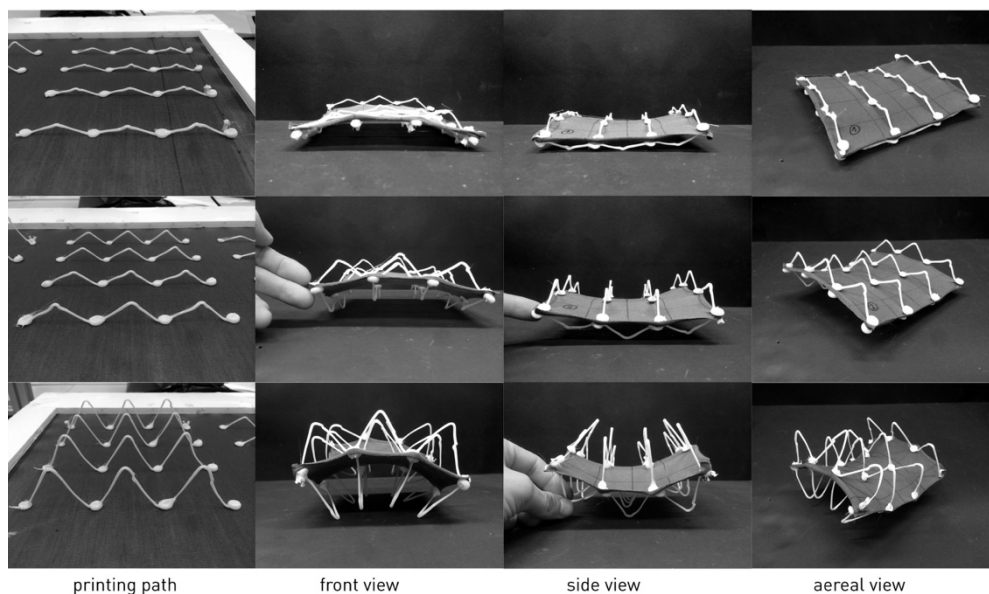


Figure 9

Samples of the anticlastic series. From top to bottom: 10 mm A_i , 20 mm A_i , 40 mm A_i .

Modeling a geometrical transformation

The first step to understand the behavior of the system was to brake it into more elementary subsystems. Accordingly, we analyzed it at several scales in parallel: as a row system (U or V), as a one-triangle-system and as a half triangle.

Dialogue of forces

The basic mechanics of the system can be analyzed at the scale of a triangle. It is observed that, when releasing the pre-stressed fabric it exerts a tension force between

the contact points that is a function of its hyperelastic behavior. This force is taken by the filament partly in bending (tangential force) and partly in compression (radial force). Furthermore, the bending stiffness of the filament is a function of its section's diameter and the length of the “arms” of the triangle. Finally, the amount of forces taken in compression or bending will be in relation to the initial angle between the filament and the fabric [fig. 10].

Geometrical model

As a row system, the discretized curvature of the fabric is produced by the contribution of the rotation and deformation of each triangle of the row. Consequently, since each triangle is symmetric, their contribution to the curvature is also assumed symmetric on their two contact points, therefore the variations on the curvature would be a function of the difference on the Initial Amplitude of each triangle.

In order to generate the geometrical model of the transformation [fig. 10], some assumptions were made:

1. All triangles with the base on the fabric are symmetrical.
2. Filament diameter is constant.
3. Each vertex of the triangle is a hinge that rotates around an axe normal to the plane of the triangle.
4. The rotation arms are infinitely stiff and any shortening due to bending is negligible.
5. $\gamma_i = 180^\circ$
6. $\gamma_f = \gamma_i - (\beta_{01} + \beta_{12})$
7. $\{01\}$ rotates to position $\{01'\}$ following a circle of R radius with center in $\{1\}$
8. $F_i \geq F_f$ and $F_i = F_f$ if $A_i = 0$
9. $A_i \leq A_f$ and $A_i = A_f$ if $A_i = 0$
10. $\beta_i = 0$

Transformation functions

From data analysis we could state that there is a function relating the Initial Amplitude (A_i) with the ratio between the Initial Frequency (F_i) and the Final Frequency (F_f) (1). At the same time, it was observed that another function of the F_i/F_f ratio (corresponding to the stretching of the fabric during the transformation) defines the theoretical β_f angle (rotation angle), therefore, the curvature (2).

$$f A_i = F_i / F_f \quad (1)$$

$$f F_i / F_f = \beta_f \quad (2)$$

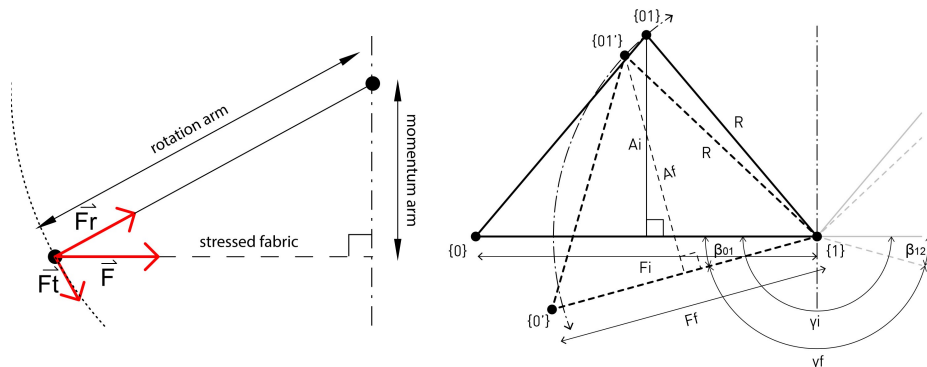


Figure 10

Left: forces scheme; right: geometrical transformation model.

Once obtained the F_i/F_f ratios and the theoretical β_f , we made two charts [fig. 11] relating the variables of the functions (1) and (2) presented above. From those charts, the trendlines of the data were identified and the quadratic functions of those curves extracted. These two functions (3) and (4) are the key that later enabled the computational tools to predict and simulate STH behavior.

$$F_i/F_f = 0.0002 A_i^2 + 0.0024 A_i + 1.0015 \quad (3)$$

$$\beta_f = \sqrt{\frac{F_i}{0.0009 F_f} - 1111.8858} - 1.0555 \quad (4)$$

A preliminary Computational Design tools workflow

As mentioned before, when aiming to explore the design potential of the STH technique, it's relevant to test it solving *forward problems* as well as *inverse problems*, hence the workflow proposed is a prediction-design-fabrication-simulation one [fig. 11]. Together with the fabrication algorithm that sets up the robot printing path, the Computational Design tools developed were a Print Path Generator, a Form-finding tool and a Print Path Designer. For further developments at architectural scale, a Finite Element Analysis tool should be implemented as part of the workflow.

Since the focus of this paper is on presenting the logic of translation from material behavior phenomena into Computational Design environment, we will only introduce one of the preliminary tools as a proof of concept.

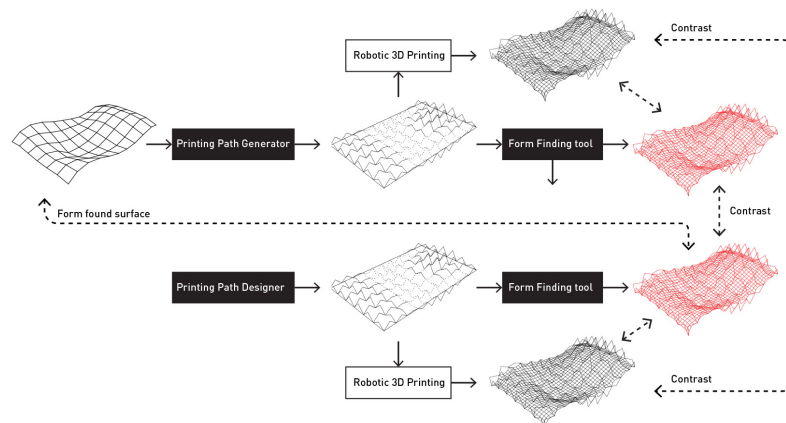


Figure 11
Proposed Computational Design workflow

Print Path Generator (PPG)

This tool is aimed to analyze an inputted 2.5D surface for generating the robotic print path that would lead to an STH “version” of it. Since STH were developed under a very restricted scenario (only one design variable), its formal repertoire remains limited. This implies that not every 2.5D surface can be reproduced with this technique. Further explorations on non-square initial grids could lead to a further extension of the formal lexicon.

Similarly to the other computational tools developed, the PPG was developed in Rhino 5 environment. It combines Grasshopper components, GhPython and C#¹. It's workflow is presented on figure 12.

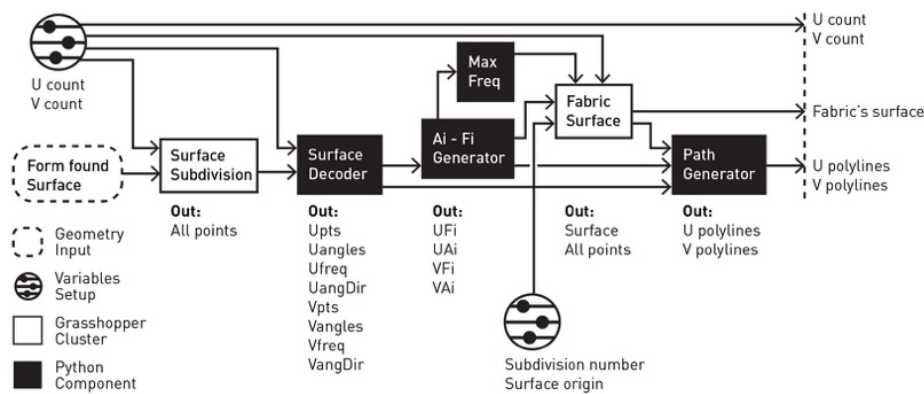


Figure 12
Computational workflow for the Printing Path Generator tool.

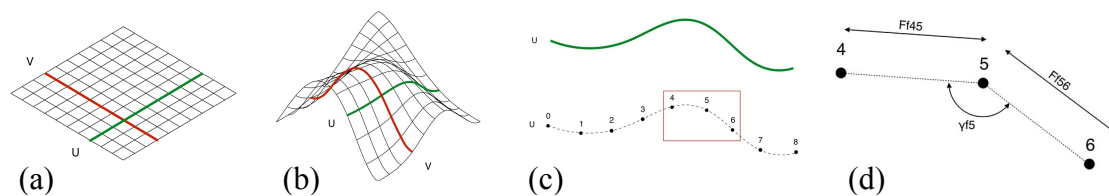


Figure 13
Surface decoding process. From left to right: flat surface, deformed surface inputted, line discretization and data gathered.

This tool was tested with a series of 2.5D surfaces manually deformed from a flat surface to obtain double curvature ones. The printing paths generated by the PPG were consequently tested with the Form-finding Tool developed where it was observed that, in general terms, the predicted path was producing a transformation in the targeted direction, although the amount of local curvature was not exactly the same as the original surface. Here the discrepancies could have occur due to:

1. the original surface wasn't informed by the restrictions of the STH systems, so an arbitrary surface always will be a "translation".
2. the Form-finding tool has a "shear" component that forces the triangles to be in a plane, therefore inducing a degree of distortions on the simulation. This issue should be addressed on a revision of this tool.

¹ Sorting Points Component in C# developed by Daniel Piker. Downloaded from: <http://www.grasshopper3d.com/forum/topics/kangaroo-bending-1>. Visited on August 10th, 2016, 9:05 pm.

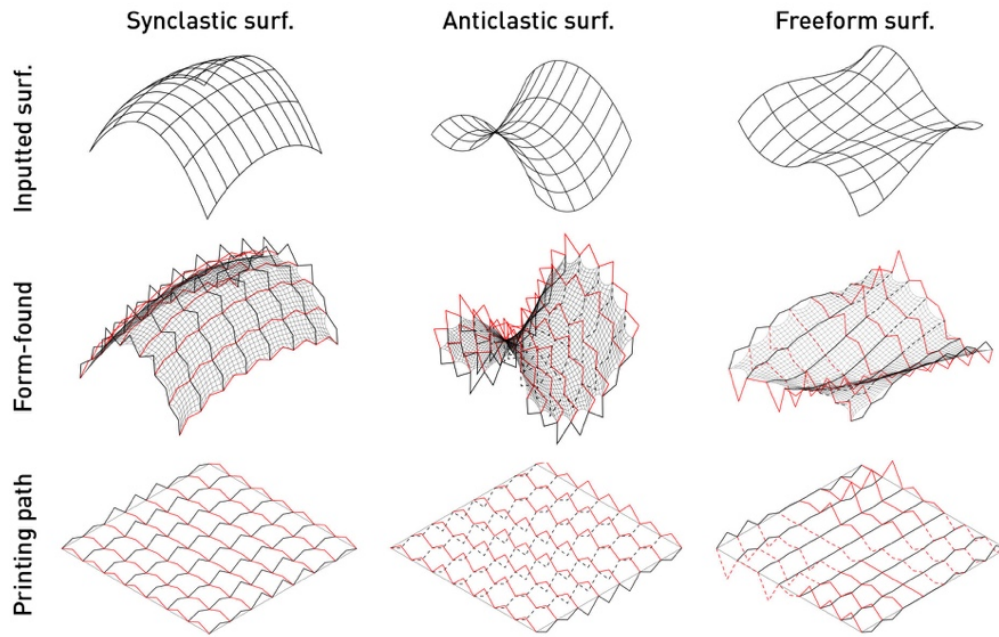


Figure 15
Comparison between the inputted surface and the form-found simulation produced from the print path generated by the Print Path Generator.

Physical and Digital samples comparison

Due to the “in progress” character of this research, the contrast of the PPG predicted print paths with physical samples is missing. Only one series of physical samples was produced from the print paths generated by the Printing Path Designer tool (not presented here) testing synclastic, anticlastic and freeform surfaces. Nevertheless, these samples were variants of the same topologies tested with the PPG and they served to test the reliability of the Form-finding simulations. Although some discrepancies were appreciated, in general terms, the transformations occurred in the predicted direction, making us optimistic regarding a future revision of the current tools and procedures.

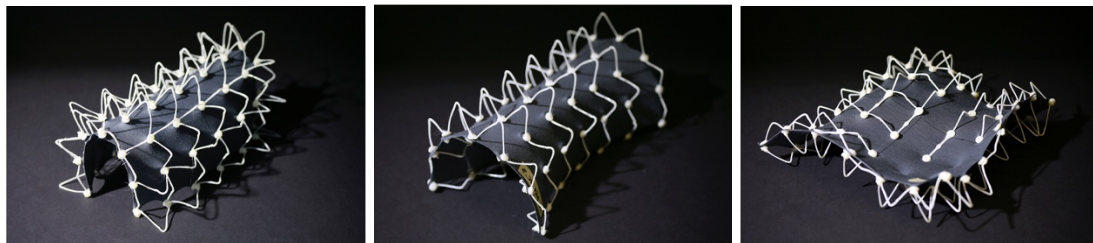


Figure 16
Physical samples printed from Printing Path Designer tool. Left to right: synclastic surface, anticlastic surface, freeform surface.

Conclusions

This paper introduced Spatial Textile Hybrids; a novel technique for generating textile hybrid systems by actuating pre-stressed fabrics with robotically 3D printed ABS filament. A revision of the process of comprehension of their material behavior, formulation of a transformation hypothesis and the capture of the necessary data for the parametrization of the system was exposed. Finally, an example of a computational design application of this technique was presented in order to illustrate the potential that Spatial Textile Hybrids might have for designers.

References

- Raviv, D., Zhao, W., McKnelly, C., Papadopoulou, A., Kadambi, A., Shi, B., Hirsch, S., Dikovsky, D., Zyracki, M., Olguin, C., Raskar, R., Tibbits, S. “Active Printed Materials for Complex Self-Evolving Deformations”, in *Scientific Reports*, vol. 4, num. 7422, pp. 1-8, 2014.
- Lienhard, J., Ahlquist, S., Menges, A., Knippers, J. “Extending the Functional and Formal vocabulary of tensile membrane structures through the interaction with bending-active elements” in *Re-Thinking lightweight structures, Proceedings of Tensinet Symposium*, Istanbul, 2013.
- Ahlquist, S., Menges, A., “Frameworks for Computational Design of Textile Micro-Architectures and Material Behavior in Forming Complex Force-active Structures” in Beesley, P., Kahn, O., Stacey, M. (eds.) *ACADIA 2013 Adaptive Architecture: Proceedings of the 33rd Annual Conference of the Association for Computer Aided Design in Architecture*, pp. 281-292, Cambridge, Ontario, 2013.
- Gladman, S., Matsumoto, E., Nuzzo, R., Mahadevan, L., Lewis, J. “Biomimetic 4D printing” in *Nature Materials* 15, pp. 413-418, 2016.
- Tibbits, S., McKnelly, C., Olguin, C., Dikovsky, D., Hirsch, S. “4D Printing and Universal Transformation” in Gerber, D., Huang, A., Sanchez, J. (eds.) *ACADIA 2014 Design Agency: Proceedings of the 34th Annual Conference of the Association for Computer Aided Design in Architecture*, pp. 539-548, Los Angeles, 2014.